

Article

Lipozyme[®] TL IM Biocatalyst for Castor Oil FAME and Triacetin Production by Interesterification: Activity, Stability, and Kinetics

Alba Gómez-Calvo¹, M. Esther Gallardo^{2,*}  and Miguel Ladero^{1,*} 

¹ FQPIMA Group, Materials and Chemical Engineering Department, Chemical Sciences School, Complutense University of Madrid, 28040 Madrid, Spain

² Translational Research with IPS Cells Group, Hospital 12 de Octubre Research Institute, 28041 Madrid, Spain

* Correspondence: egallardo.imas12@h12o.es (M.E.G.); mladerog@ucm.es (M.L.)

Abstract: Global climate change and present geopolitical tensions call for novel, renewable, and, ideally, sustainable resources and processes that, in the end, will be integrated in the natural cycles of carbon and water, progressively replacing non-renewable feedstocks. In this context, the production of biofuels and, in consequence, of biodiesel plays a notable role. This work is focused on the production of fatty acid methyl esters (FAME) from castor oil, an abundant non-edible oil, using a sustainable technology approach based on industrial lipases and methyl acetate as a methylating reagent to reduce biocatalyst inactivation. We have selected a stable industrial enzyme preparation to determine its suitability for FAME production: Lipozyme[®] TL IM (an inexpensive lipase from *Thermomyces lanuginosus* immobilized by agglomeration in silica gel). Several operational variables affecting the enzyme activity have been studied: methanol excess (6:1 to 13:1), temperature (from 40 to 60 °C), and enzyme concentration (10 and 30% *w/w*). At all temperatures and reagent ratios, we have also tested the enzyme stability for six cycles, showing its low to negligible inactivation under operational conditions. Finally, a novel multivariable kinetic model has been proposed and fitted to experimental data obtained in a wide experimental range for the first time, showing that direct and reverse in-series reactions are present. We have estimated the values of the kinetic constants and their standard errors, and goodness-of-fit parameters, observing that the kinetic model fitted very reasonably to all retrieved experimental data at the same time.

Keywords: castor oil; FAME; ricinoleic acid; lipase; screening; kinetic model



Citation: Gómez-Calvo, A.; Gallardo, M.E.; Ladero, M. Lipozyme[®] TL IM Biocatalyst for Castor Oil FAME and Triacetin Production by Interesterification: Activity, Stability, and Kinetics. *Catalysts* **2022**, *12*, 1673. <https://doi.org/10.3390/catal12121673>

Academic Editors: Hwai Chyuan Ong, Chia-Hung Su and Hoang Chinh Nguyen

Received: 11 November 2022

Accepted: 15 December 2022

Published: 19 December 2022

Publisher's Note: MDPI stays neutral with regard to jurisdictional claims in published maps and institutional affiliations.



Copyright: © 2022 by the authors. Licensee MDPI, Basel, Switzerland. This article is an open access article distributed under the terms and conditions of the Creative Commons Attribution (CC BY) license (<https://creativecommons.org/licenses/by/4.0/>).

1. Introduction

Global warming will raise the average world temperature by 1.5 °C in the period from 2030 to 2052, as indicated in the IPCC Special Report on the effects that this temperature increase will have on our planet. In this situation, a quick transition to zero- or low-carbon economies would save trillions of USD: 149.78–791.98 trillion USD is the expected cost for the current energy scenario if it is maintained till 2100, a cost that can be avoided if all countries follow a self-preservation strategy to reach a temperature change well below 2 °C or 1.5 °C in this period [1]. For such purpose, a circular economy (CE) advocates for decoupling economic growth and our energy and material requirements, thus avoiding further environmental degradation [2]. Within this context, industrial ecology proposes to close geochemical material cycles, in particular the carbon cycle, integrating human industrial activities in these natural cycles [3]. Moreover, we need to integrate our activities not only in the geochemical material cycles (carbon, nitrogen, and water) but also in the global energy cycle. Considering that all natural energy inputs (almost all due to solar irradiation, a small part due to Earth's heat and tides) are five orders of magnitude higher than our own technical needs and all energy losses and natural needs of the planet, enough solar energy can be derived to cover human needs by 2100 [2].

The production of biofuels, and biodiesel in particular, is one of the industrial strategies to integrate energy obtention into the geochemical cycles [4]. In the case of biodiesel, the usual raw materials are edible oils (palm, soybean, and sunflower . . .), so, as in other first generation biorefineries, a competition is created between the food and energy sectors, with complex logistical and ethical consequences. As a way to decouple energy creation and food supply, we need to use more abundant feedstock of lignocellulosic and an algae-like nature, developing novel processes within second to fourth generation biorefineries [4–6]. A second biorefinery oil crop is castor oil coming from *Ricinus communis*, a shrubby plant of the family *Euphorbiaceae* able to grow in semi-arid lands and with a high oil productivity per hectare (half that of oil palm) [7].

Fatty acid methyl esters (FAME), the main ingredients of biodiesel, are obtained by the transesterification of alcohols and triglycerides in diverse conditions. Supercritical processes can be conducted at high pressure (9–200 atm) and temperature (80–300 °C) in the absence of any catalyst, or in the presence of basic catalysts, with side esterification of any present fatty acid being catalyzed by acids in 10–60 min for harsh conditions or up to 8 h for the mildest one [4]. In these conditions, FAME yields are in the 92–100% range. Even milder conditions can be achieved with free and immobilized lipases: 35–50 °C for 8–72 h will produce a 78–97% FAME yield. The lipase biocatalysts have a brilliant future if mass-transfer limitations and enzyme innate instability issues are overcome at affordable costs, as they accept all type of triglyceride and fatty-acid rich mixtures, including highly acidic cheap waste oils [4,8] and can be combined to control selectivity issues [9].

The selection of a given raw material is of key importance depending on the FAME final use. It can account for up to 60–70% of the operational costs (OPEX) of a biodiesel plant [10]. Castor oil is rich in ricinoleic acid, an acid with a secondary hydroxyl group in C12 relatively next to the carbon-carbon double bond at C9-10. This functional group explains the solubility of the fatty acid in alcohols and its higher innate interactions resulting in increased viscosity in comparison to other long fatty acids. This higher viscosity of castor oil affects the biodiesel obtained from its transesterification with short-chain alcohols and provides the need for blending it with diesel, other biodiesel and/or viscosity ingredients to comply with international standards, such as ASTM D6751 and EN 14214 [7]. The solubility of castor oil in methanol and ethanol reduces the usual limitations to productivity posed by liquid-liquid mass transfer in acid-base processes (30–360 min, 85–99% FAME yield) and using lipases (8 h, 84% FAME yield) [7,11]. Regarding lipase stability, methanol progressive addition (batch-fed) is recommended to avoid lipase inactivation. A second option is to use other alcohols as acyl acceptors: ethanol, 2-butanol, or even esters such as methyl and ethyl acetate, using interesterification reactions between esters instead of the more common transesterification processes. These reactions are in equilibrium as indicated in Figure 1. The use of acetates dramatically increases the stability of immobilized lipases, allowing for their use with no inactivation for as much as 100 cycles [8]. In addition, the use of optimal immobilization procedures increases the enzyme stability even more [12,13].

Apart from the application in the bioenergy sector, FAMEs from castor oil are valuable in the chemical industry and other related sectors as a source of bio-lubricants essentially composed by monoricinolein and diricinolein [14,15], polyesters and polyurethanes [7,16], plasticizers [17], and the ricinoleic acid itself [18]. On its part, triacetin is a notable plasticizer, emulsifier, humectant, and fuel additive, so this compound encounters diverse applications in several sectors: energy, polymers, cosmetics, pharma, and food [19]. In fact, in the production of biodiesel, glycerol is sometimes an undesirable by-product. To avoid its formation, interesterification reactions with acetates produce triacetin. This compound can be mixed with FAMEs in a 10% *w/w* proportion, complying with international biodiesel standards, avoiding the formation of glycerol and its costly purification [20].

Considering more high-value applications, castor oil is an ancient, well-known laxative used in small doses to alleviate gastrointestinal disorders [21]. The presence of several functional groups in ricinoleic acid and its esters allows for wide range of possible reactions: pyrolysis, oxidation, urethane production, glycosylation, esterification, epoxidation, saponi-

fication, and amidation, to name the main ones [22]. This rich array of chemical possibilities explains the plethora of applications in diverse sectors, including the high-value bioactive derivatives in the pharma industry. Several ricinoleic acid amides have shown powerful *in vitro* antiproliferative activity, in particular against glioma cell lines [22,23]. Methyl ricinoleates (the most abundant FAMES from castor oil) are a fine starting point for the synthesis of amides and other derivatives, given the trend of the acid to form estolides [22]. In this way, diverse acetates of this acid have been synthesized and probed against several cell lines, showing their potential [24]. Castor oil itself is also a good raw material for the synthesis of ricinoleic vanillyl ester, a compound with a notable activity as an antioxidant and antibacterial agent [25]. Complex chemicals such as 1-O-alkylglycerols of the acid with methoxy, gem-difluoro, azide, and the hydroxy group at position 12 of the alkyl chain, were recently synthesized and combined with diverse well-known antibiotics, being the hydroxyl derivative the most active as an antimicrobial agent in these mixtures when used alone. The most promising fact was that several antibiotic-ricinoleic acid derivative combinations showed a powerful positive synergy, increasing the antimicrobial activity up to four-fold in comparison to the antibiotic alone [26]. Most promising antimicrobial and antifungal activities have also been demonstrated for ricinoleic acid-based lipoamino acid derivatives, specifically against various *Candida* strains [27]. In the cutting-edge biomedical field of personalized medicine, based on diverse types of stem cells including human induced pluripotent stem cells (hiPSCs), castor oil is finding novel applications through the synthesis of diverse biomaterials based on its polyurethanes. For example, low-cost scaffolds to avoid oxidative stress of the stem cells during wound healing are most promising [28]. Moreover, stem cells can be differentiated to skeletal muscle, cardiomyocytes, neurons, and osteogenic lineages by applying specific external electric fields. In this sense, electroactive polyurethane/siloxane scaffolds derived from castor oil have also been synthesized and tested for cardiac patches [29].

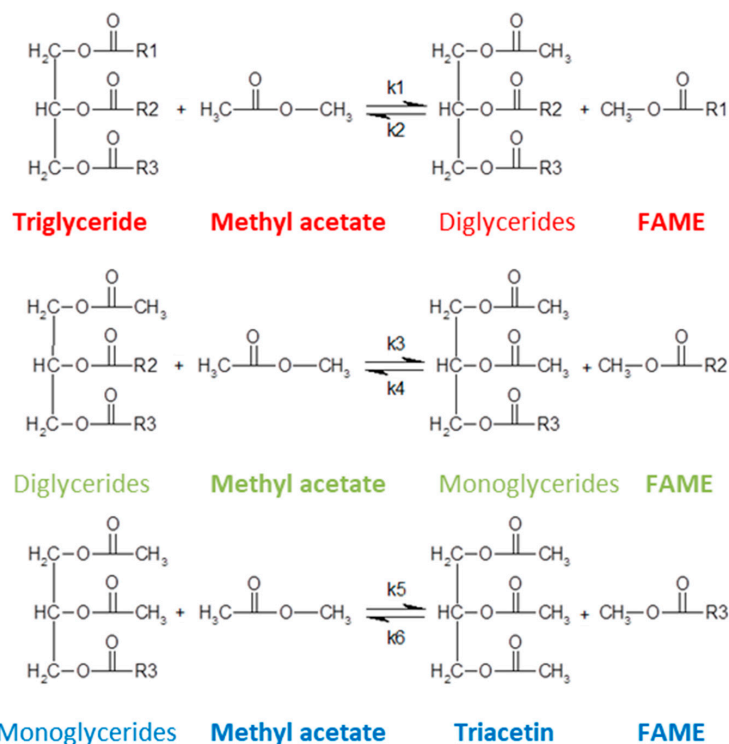


Figure 1. Simplified reaction network or scheme for the transesterification process of methyl acetate and triglycerides from castor oil: triglycerides are transformed into 1,2 and 1,3 diglycerides (grouped as diglycerides) and FAMES; diglycerides are the source of 1- and 2-monoglycerides and FAMES. These, in turn, react with more methyl acetate to obtain triacetin and more FAMES. All these consecutive reactions are transesterifications catalyzed by Lipozyme[®] TL IM.

The aim of this work is to study the interesterification of castor oil with methyl acetate to obtain a mixture of triacetin and FAMES of ricinoleic acid. For that purpose, we have selected a very stable immobilized lipase preparation manufactured by Novozymes A/S: Lipozyme TL IM. Its activity and stability have been assessed firstly in diverse operational conditions. In the most relevant conditions, ensuring the enzyme stability, an in-depth kinetic study was performed proposing a scheme of interesterification reactions, and fitting a set of differential equations for the rates of the direct and inverse reactions in such network to all data obtained in a wide operational range.

2. Results

2.1. Effect of Operational Conditions on Yield and Activity

To establish an accurate kinetic model for the interesterification reaction between methyl acetate and the triglycerides in castor oil, we have performed twelve 24-h runs in triplicate. Table 1 compiles the conditions of all runs together with initial reaction rates, triglyceride conversion at 24 h and FAME yield at that same reaction time, while Figure 2 shows the effect of substrate molar ratio, temperature, and enzyme concentration on triglyceride conversion at 24 h and initial reaction rate (r_0).

Table 1. Experimental runs of the interesterification of methyl acetate with castor oil: conditions and key process parameters, triglyceride conversion, FAME yield at 24 h and initial reaction rate (r_0).

Run	Enzyme Concentration (%) <i>w/w of Oil</i>	Temperature (°C)	Substrate Molar Ratio	TG Conversion (24 h)	FAME Yield (24 h)	$r_0 \times 10^6$ (mol/(L·s))
E1	10	40	1:06	0.67	0.35	5.72
E2	10	40	1:13	0.71	0.37	4.13
E3	10	50	1:06	0.77	0.42	7.62
E4	10	50	1:13	0.89	0.55	6.19
E5	10	60	1:06	0.85	0.5	8.58
E6	10	60	1:13	0.87	0.52	8.25
E7	30	40	1:06	0.88	0.54	19.06
E8	30	40	1:13	0.88	0.59	17.88
E9	30	50	1:06	0.91	0.6	24.77
E10	30	50	1:13	0.93	0.64	20.63
E11	30	60	1:06	0.91	0.64	30.49
E12	30	60	1:13	0.97	0.71	23.38

We can see that triglyceride conversion increases with temperature, reaching values as high as 97% at 60 °C, with the highest excess of methyl acetate and a high enzyme concentration, while FAME yield in these conditions is 71%. Therefore, reactors featuring an elevated concentration of this biocatalyst could be adequate for the process (i.e., fixed bed reactors, where typically a solid volume fraction in excess of 50% exists). In any case, methyl acetate should be present in a molar ratio far higher than 1:3, which is the stoichiometric ratio, to shift all equilibriums towards the products.

In contrast, we observed an incremental value for initial reaction rate, which reflects the enzyme activity, when temperature increases at all other variables constant. As expected, the enzyme activity increases proportionally to the amount of enzyme present in the reaction medium, an aspect to be considered in any proposed kinetic model. Finally, the excess of the methylating agent affects the activity negatively, thus showing the effect of a high dilution of triglycerides with methyl acetate. However, an excess of methyl acetate is needed to obtain high FAME yields.

2.2. Kinetic Modelling

A more profound study of the interesterification reactions can be done by fitting an adequate kinetic model describing the experimental results at all relevant operational conditions. For this it is essential to know the concentrations of all the compounds present in the reaction system at diverse processing time values. The progressive production of

FAMES through three reactions in-series has been previously depicted in Figure 1. It can be observed that the reactions are reversible, as all compounds involved are substrates for the lipase of *Thermomyces lanuginosus*. The initial triglycerides are transformed into FAMES and 1,2- and 1,3-diglycerides, while these last compounds react with methyl acetate to obtain 1- and 2-monoglycerides and FAMES. Finally, monoglycerides can react with more methyl acetate to liberate triacetin and FAMES.

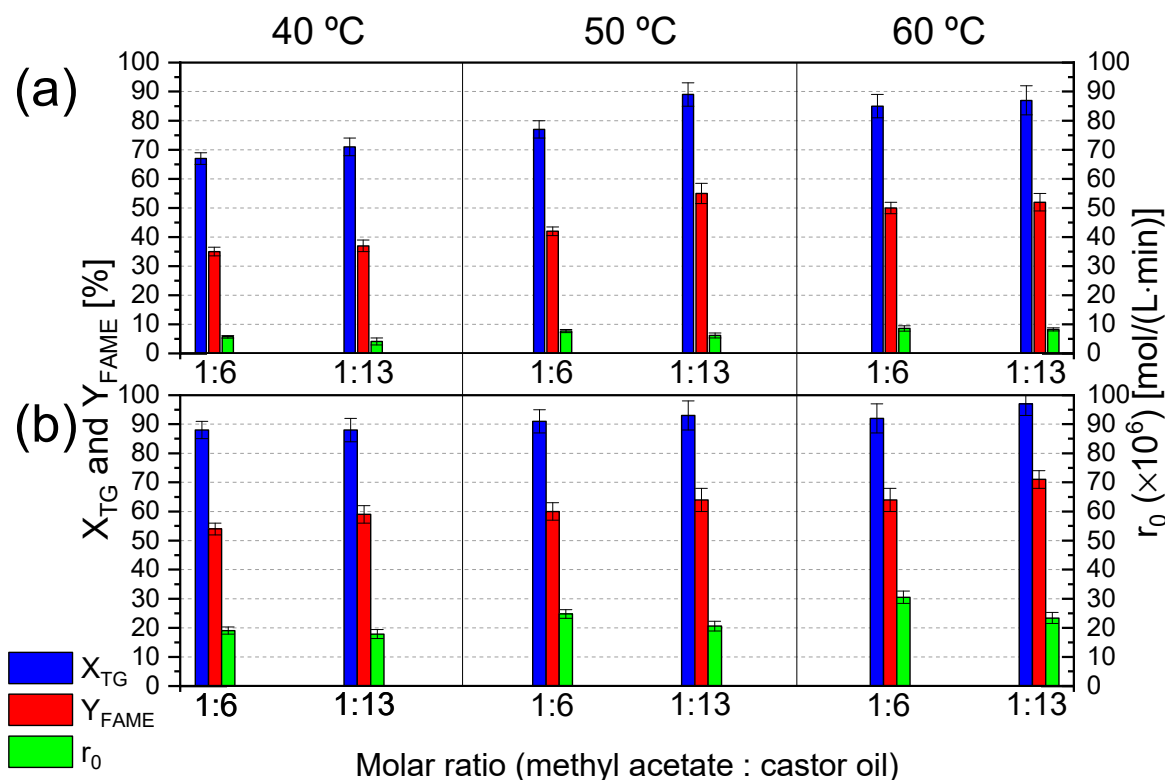


Figure 2. Effects of the main operational conditions (substrate molar ratio, temperature, and enzyme concentration) on the triglyceride in castor oil at 24 h and on the initial reaction rate (r_0) at an enzyme concentration of (a) 10% w/w oil, and (b) 30% w/w oil.

An aspect that we have observed in all 12 runs, and that is of great relevance, is how the concentrations of all the compounds stabilize with time, i.e., it tends to a horizontal asymptote, which indicates that there are apparently equilibria limitations in all reactions. This situation is taken into account in the proposed kinetic model, as the reverse reactions which slow down the production of FAMES must be taken into account.

Only some authors have proposed models and reaction orders that fit the experimental data previously obtained in their studies. In fact, there is no kinetic model for this reaction system taking into account all relevant operational variables. The only model proposed for the reaction with methyl acetate (using the *Candida antarctica* B lipase) has been proposed by Xu et al. but it is very simple and omits the effect of temperature and enzyme concentration [30]. The few models created for enzyme catalysis, in addition to being contradictory, usually describe the transesterification reaction with methanol, not the less usual interesterification process with methyl acetate. In fact, as commented, there is now a trend to use liquid enzymes to produce biodiesel from diverse oils and methanol, with the adverse effect of this alcohol on enzyme stability, an aspect that determines a progressive addition of the alcohol to the reaction medium (batch-fed operation). An in-depth kinetic model was proposed by Andrade et al. working with castor oil as a triglyceride source and with the novel enzyme preparation named Eversa Transform produced by Novozymes A/S [11]. A relatively simple kinetic model able to be fitted to data at several temperatures from 35 to 50 °C was obtained; this model was basically similar to that of Xu et al.,

where second order kinetic expressions, first-order respect to each relevant reagent, is proposed. The most relevant differences are the presence of hydrolysis reactions together with methanolysis (due to the obligations of adding water to enhance Eversa Transform activity and stability) and the applicability of the model to a wide range of operational conditions. Although some simple models have been proposed for the liquid enzyme of *Thermomyces lanuginosus* for the transesterification of triglycerides contained in phoenix tree seed oil [31], this kinetic information is scarce till now as most studies are focused on the statistical optimization of the process to maximise the yield of FAMES. For the immobilized preparation of this enzyme, Lipozyme® TL IM, there is only one relevant paper, to the best of our knowledge, based on the use of a blend of non-edible oils (castor oil is a non-edible oil, as is this mix, though the mix does not contain castor oil) and methanol [32]. These transesterifications were performed under ultrasound conditions (35 kHz) at 25–45 °C, with a molar ratio methanol:oil 4:1–11:1, and enzyme loading 1–5% *w/w* oil, using water as a viscosity enhancer, which is advantageous when using alcohols if added not in excess. While a simple pseudo-first order kinetic model (only direct reactions) was used to determine the activation energies, a more complex bi-bi ping-pong kinetic model was fitted to data obtained in three particular conditions (not giving the activation energies for a model able to be fitted to all studied conditions). Thus, it is evident that there is still a lack of a complete, multivariable kinetic model in most cases and, in particular, no kinetic model exists for the interesterification reaction network created by the biocatalyst Lipozyme® TL IM when it acts on the system of castor oil-methyl acetate in a wide interval of operational conditions. This model, based on pseudo second-order reactions, as suggested by Xu and other authors [11,30], is presented in the Equations (1)–(6).

$$\frac{dC_{TG}}{dt} = -k_1 \cdot C_E \cdot C_{TG} C_{MA} + k_2 \cdot C_E C_{DG} C_{FAME} \quad (1)$$

$$\frac{dC_{DG}}{dt} = k_1 \cdot C_E \cdot C_{TG} C_{MA} - k_2 \cdot C_E C_{DG} C_{FAME} - k_3 \cdot C_E C_{DG} C_{MA} + k_4 \cdot C_E C_{MG} C_{FAME} \quad (2)$$

$$\frac{dC_{MG}}{dt} = k_3 \cdot C_E \cdot C_{DG} \cdot C_{ACT} - k_4 \cdot C_E \cdot C_{MG} \cdot C_{FAME} - k_5 \cdot C_E \cdot C_{MG} \cdot C_{ACT} + k_6 \cdot C_E \cdot C_{TAC} \cdot C_{FAME} \quad (3)$$

$$\frac{dC_{MA}}{dt} = -k_1 \cdot C_E \cdot C_{TG} \cdot C_{MA} + k_2 \cdot C_E \cdot C_{DG} \cdot C_{FAME} - k_3 \cdot C_E \cdot C_{DG} \cdot C_{ACT} + k_4 \cdot C_E \cdot C_{MG} \cdot C_{FAME} - k_5 \cdot C_E \cdot C_{MG} \cdot C_{ACT} + k_6 \cdot C_E \cdot C_{TAC} \cdot C_{FAME} \quad (4)$$

$$\frac{dC_{FAME}}{dt} = k_1 \cdot C_E \cdot C_{TG} \cdot C_{MA} - k_2 \cdot C_E \cdot C_{DG} \cdot C_{FAME} + k_3 \cdot C_E \cdot C_{DG} \cdot C_{ACT} - k_4 \cdot C_E \cdot C_{MG} \cdot C_{FAME} + k_5 \cdot C_E \cdot C_{MG} \cdot C_{ACT} - k_6 \cdot C_E \cdot C_{TAC} \cdot C_{FAME} \quad (5)$$

$$\frac{dC_{TAC}}{dt} = k_5 \cdot C_E \cdot C_{MG} \cdot C_{ACT} - k_6 \cdot C_E \cdot C_{TAC} \cdot C_{FAME} \quad (6)$$

where k_1 to k_6 are the kinetic constants of the direct and inverse reactions (L/(mol·min)) and C_E is the enzyme concentration in g/L (65 g/L at 10% *w/w* enzyme to oil and 1:6 molar ratio; 46.7 g/L at 10% *w/w* enzyme to oil and 1:13 molar ratio; 195 g/L at 10% *w/w* enzyme to oil and 1:6 molar ratio; 140 g/L at 10% *w/w* enzyme to oil and 1:13 molar ratio). C_{TG} , C_{DG} , C_{MG} , C_{MA} , C_{FAME} and C_{TAC} refer to the concentrations of triglycerides, diglycerides, monoglycerides, methyl acetate, fatty acid methyl esters, and triacetin, respectively.

Firstly, we fitted this model using the numerical integration and non-linear regression algorithms implemented in Aspen Custom Modeler v11, as indicated in the Section 3, using only data obtained at a given temperature, that is, four runs where substrate molar ratio and enzyme concentrations vary at either 40, 50 or 60 °C. The results are collected in Table 2, finding there the kinetic parameters and their standard errors and the goodness-of-fit parameters used in this case: the sum of residual squares (SQR) and the value for the Fisher's F at 95% confidence. We can see that all kinetic constants are positive and with a low standard error, showing an incremental trend with the rise of temperature, as expected. The fittings, considering the low values of SQR and very high values of the Fisher's F

(over the 20–30 threshold value), indicate that the model fits very reasonably with the experimental data.

Table 2. Kinetic constants from runs at constant temperatures with their standard errors and goodness-of-fit parameters.

T (°C)	$k_1 (\times 10^4)$ (l ² /mol·g _E ·h)	$k_2 (\times 10^4)$ (l ² /mol·g _E ·h)	$k_3 (\times 10^4)$ (l ² /mol·g _E ·h)	$k_4 (\times 10^4)$ (l ² /mol·g _E ·h)	$k_5 (\times 10^4)$ (l ² /mol·g _E ·h)	$k_6 (\times 10^4)$ (l ² /mol·g _E ·h)	SQR	F
40	2.36 ± 0.03	2.30 ± 0.27	1.49 ± 0.06	4.39 ± 0.50	0.57 ± 0.07	2.87 ± 0.61	0.023	4.93 × 10 ⁵
50	3.69 ± 0.07	2.58 ± 0.64	2.33 ± 0.11	5.72 ± 1.26	1.69 ± 0.22	3.14 ± 0.91	0.020	2.58 × 10 ⁵
60	4.57 ± 0.09	3.11 ± 0.40	2.65 ± 0.11	5.88 ± 0.69	2.07 ± 0.14	3.71 ± 0.70	0.035	1.82 × 10 ⁵

In a second step, a linearised version of the Arrhenius equation (Equation (7)) was utilized to obtain initial values for the neperian of the preexponential term of such equation for each kinetic constant ($\ln k_{i0}$) and the activation energy for such constant (E_a). The application of this equation is observed in Figure 3, where we can also observe the values retrieved for all relevant parameters and the fine fitting of the equation, in most cases. These values of $\ln k_{i0}$ and E_a were the starting point for the multivariable fitting of the kinetic model to all experimental data, thus using temperature, enzyme concentration, and time as independent variables, affecting the temporal evolution of the concentrations of all compounds involved in the reactions.

$$\ln k_i = \ln k_{i0} - \frac{E_a}{RT} \quad (7)$$

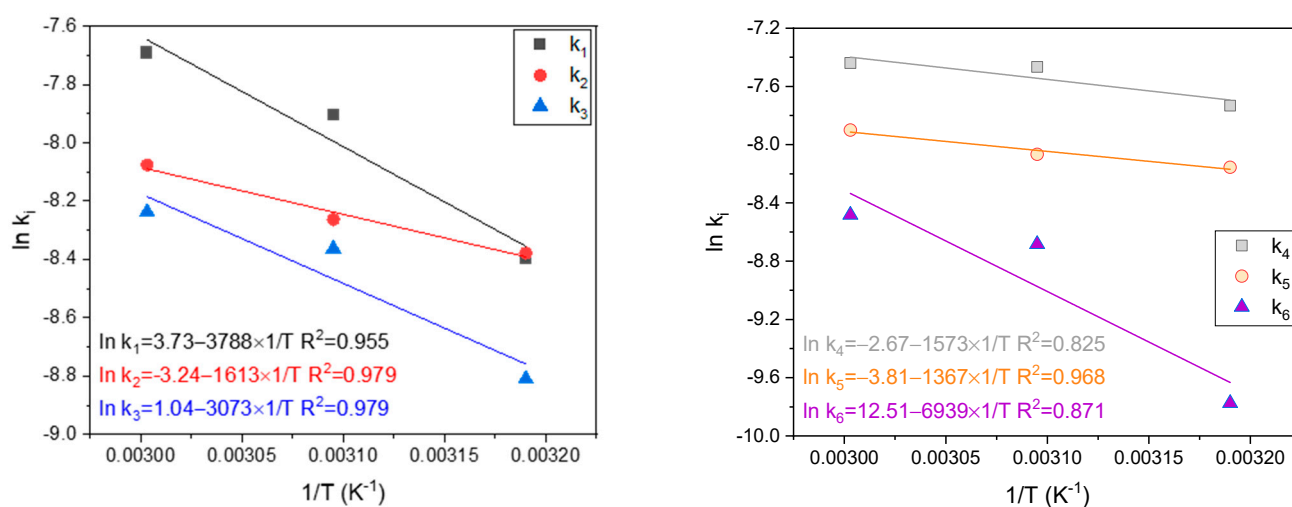


Figure 3. Estimation of $\ln k_{i0}$ (point of intersection of each line on the ordinate axis) and E_a/R (slope of each line) by linearising the Arrhenius equation applied to the kinetic constants of the proposed model.

The kinetic constants, as functions of temperature, are shown in Table 3 together with their standard errors and SQR and the F-value. Again, standard errors are much lower than the kinetic parameter values, while SQR values are low and F-values very high; much higher than the threshold values for 95% confidence. The values of the activation energies are within the 2–150 kJ/mol that we can observe in most reaction kinetic constants. Therefore, all physical and statistical criteria advocate for the high adequacy of the proposed kinetic model under the experimental conditions studied here. As an example of the kinetic equations of the model, Equation (8) reflects the evolution of FAME concentration with the time of reaction, while, in Figure 4, we can appreciate the good fitting of the model to all relevant compounds for several runs at all temperature values, and selected TG:MA molar ratios and enzyme concentrations.

Table 3. Kinetic constants and goodness-of-fit statistical data at 95% confidence for the proposed kinetic model to fit to the interesterification of methyl acetate and castor oil triglycerides data (fitting the model to all retrieved data).

k_i ($l^2/(mol \cdot g_E \cdot h)$)	$\ln k_{i0}$	E_a/R (K)	E_a (kJ/mol)
k_1	3.21 ± 0.01	3618.0 ± 3.23	30.08 ± 0.03
k_2	-4.72 ± 0.10	1200.0 ± 33.63	9.98 ± 0.28
k_3	-0.07 ± 0.02	2724.16 ± 7.77	22.65 ± 0.06
k_4	-6.09 ± 0.07	483.19 ± 22.83	4.02 ± 0.19
k_5	3.86 ± 0.06	4244.81 ± 19.67	35.29 ± 0.16
k_6	-4.76 ± 0.16	1100.0 ± 53.90	9.15 ± 0.45
SQR		0.028	
F		753,000	

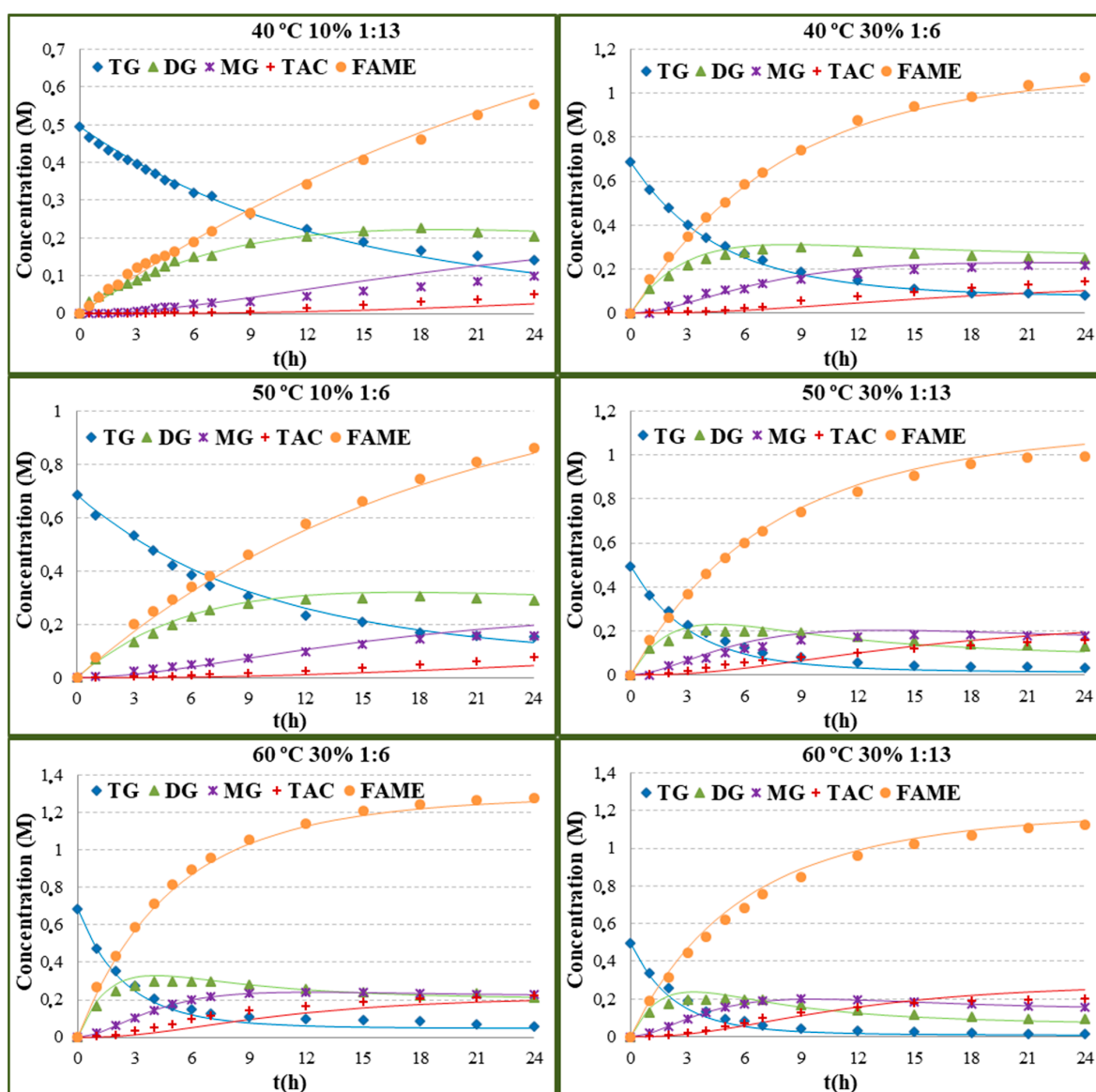


Figure 4. Fitting of the kinetic model to data of several selected methyl acetate-castor oil triglycerides interesterification runs (run details in each subfigure title: temperature $^{\circ}C$ -, percentage of enzyme per mass castor oil and molar ratio castor oil:triacetin). The fitting was performed to data from all 12 runs at the same time.

It can be appreciated that the activation energies are relatively high for the direct reactions and low for the inverse ones. These activation energies are notably lower than the ones found with pseudo-first order kinetic models for FAME production, which is about 51 kJ/mol using this same enzyme preparation for the transesterification of oils with methanol in the presence of tert-butanol [33]. Under sonication conditions, with and without water, this same parameter varies between 78.7 and 124.4 kJ/mol while for other oils, enzyme preparations and reactor configurations, it can be as low as 14.73 kJ/mol [32]. Therefore, we can suspect that internal mass transfer limitations are not very relevant in this case, as activation energies are far higher than the usual for fickian diffusion mass transfer (about 2 kJ/mol).

The evolution of all compounds indicates that, even at the highest molar ratio TG:MA (thus, the highest excess of methyl acetate) and the highest concentration of enzyme, monoglyceride concentration is not negligible. As a consequence, higher excesses of the methylating agent and higher concentrations of enzyme (found in fixed-bed reactors) should be considered to avoid the concentration of di- and mono-glycerides with the aim to meet biodiesel international standards.

$$r_{FAME} = \left(24.88 - \frac{3618}{T}\right) \cdot C_E \cdot C_{TG} \cdot C_{MA} - \left(0.0088 - \frac{1200}{T}\right) \cdot C_E \cdot C_{DG} \cdot C_{FAME} + \left(0.93 - \frac{2724}{T}\right) \cdot C_E \cdot C_{DG} \cdot C_{ACT} - \left(0.0023 - \frac{483}{T}\right) \cdot C_E \cdot C_{MG} \cdot C_{FAME} + \left(47.37 - \frac{4245}{T}\right) \cdot C_E \cdot C_{MG} \cdot C_{ACT} - \left(0.0085 - \frac{1100}{T}\right) \cdot C_E \cdot C_{TAC} \cdot C_{FAME} \quad (8)$$

Although it is complex to compare enzyme activities in biodiesel processes due to the diversity of reactions (esterification, transesterification, and interesterification processes), sources of triglycerides, and operational conditions, several lipases have been tested for biodiesel production, comparing yield to FAMEs in optimal conditions [4]. As for the enzyme activity, it can be estimated in terms of initial reaction rate (r_0) for the reaction of triglycerides. The Eversa Transform 2.0 liquid lipase preparation by Novozymes A/S showed values in the interval between 1–4 mM/min for the transesterification of refined palm oil with methanol with diverse concentrations of free fatty acids (so esterification reactions were also present) at 40 °C, 0.2 wt% of free lipase, and 2 wt% of added water [34]. When conducting transesterification reactions between phoenix tree seed oil triglycerides and methanol, the values of this parameter for Lipozyme TL100, CALA (*Candida antarctica* lipase A), and CALB (*Candida antarctica* lipase B), all liquid enzyme preparations from Novozymes A/S, were 4.6, 2.6, and 2.3 mM/min, respectively, with a 1:5 (mol/mol) substrate ratio, and 8% (*v/v*) lipase load with the enzymes working at 40 °C [31]. The transesterification of castor oil triglycerides with methanol at 35 °C, 5% *w/w* enzymes, 5% *w/w* water, and a 6 alcohol-to-oil molar ratio, using Eversa Transform 2.0, yielded a r_0 value of circa 40 mM/min [11]. In this work, the initial reaction rate fluctuated between 0.3 and 2.4 mM/min for temperatures between 40 and 60 °C, 6 to 13 methyl acetate-to-oil molar ratios, and enzyme concentrations between 10 and 30% *w/w* of castor oil.

2.3. Biocatalyst Operational Stability

As the use of methyl acetate as a methylating agent or the presence of cosolvents like tert-butanol usually results in a higher stability of the enzymatic biocatalyst [8,33], we perform several 24-h runs at all temperatures studied here, fixing the molar ratio of methyl acetate to triglyceride as 13 and the percentual enzyme concentration in 30% *w/w* oil. The results are shown in Figure 5 as the residual activity (calculated as the ratio of the initial reaction rate for any cycle to the same parameter for the first cycle at a given temperature). We can observe that, for 5 cycles at any temperature, the activity only reduces slightly, thus showing that the reaction media can stabilise the biocatalyst under working conditions. When comparing these results to those of Liu et al. [33], we can find that tert-butanol is also a stabilizing agent, with a similar behaviour but, in this case, protects the enzymes from the action of methanol as an inactivation agent. This inactivation activity of methanol under sonication conditions, and for Lipozyme[®] TL IM can be well appreciated in the work of

Malani et al. [32], where the residual activity drops to 0.1–0.3 in six cycles without buffer washing, with and without added water.

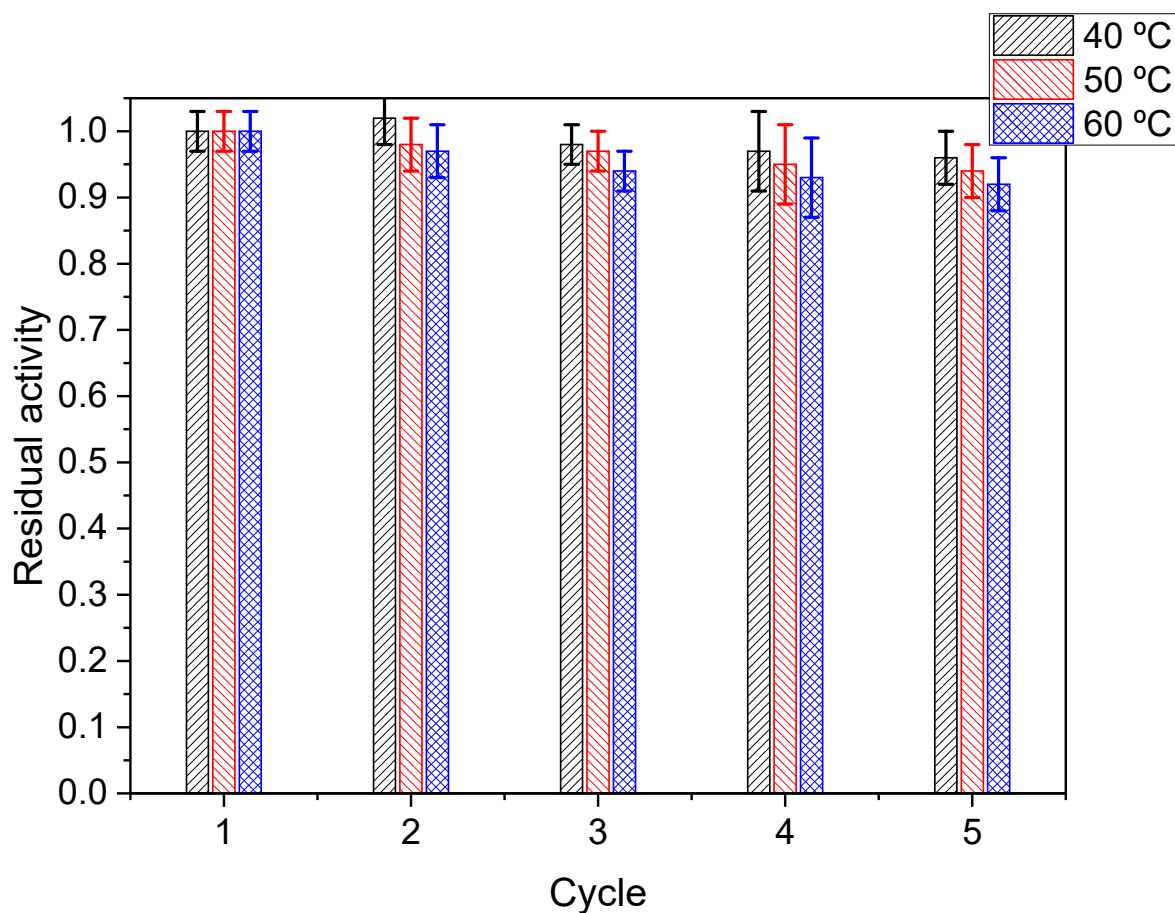


Figure 5. Evolution of the residual activity of Lipozyme® TL IM at 40, 50 and 60 °C for five consecutive reaction cycles. Fixed conditions: TG to MA molar ratio 1:13, enzyme percentual concentration 30% ($C_E = 140$ g/L).

3. Materials and Methods

3.1. Materials

Lipozyme® TL IM (a 1,3 specific lipase from *Thermomyces lanuginosus* immobilized on a non-compressible silica gel carrier) was a kind gift of Novozymes A/S (Bagsværd, Denmark). According to the manufacturer, Lipozyme® TL IM is a very effective catalyst for interesterification and can rearrange fatty acids preferentially, but not uniquely, in the 1- and 3-positions of the triglycerides. Refined castor oil was purchased by Manuel Riesgo S.A. (Madrid, Spain). Fisher Scientific UK Ltd. (Loughborough, UK) supplied methyl acetate HPLC grade. This company also supplied all RP-HPLC grade eluents: acetonitrile gradient grade, hexane, and isopropanol.

3.2. Methods

3.2.1. Enzymatic Interesterification of Castor Oil and Methyl Acetate

Several runs were performed at 40, 50 and 60 °C. In every run, we mixed 10 g of castor oil with methyl acetate so the methyl acetate:castor oil molar ratio is either 6:1 or 13:1. The reagents are added to an Erlenmeyer flask placed in a thermostatic bath and the first sample is withdrawn (zero time). After 10 mins, necessary for the reagents to reach the reaction temperature, the enzyme is added to the mixture at 20% or 30% *w/w* with respect to the castor oil. This addition of the enzyme is the zero time for any run. During the first 2 h, a sample is taken every 30 min. During the next 5 h, every hour. From 7 h onwards,

samples will only be taken every 3 h. The experiments have been carried out in duplicate and with a time lag of six hours in order to observe the complete evolution during the 24 h of the reaction. We are taking a greater number of samples during the first two hours of the reaction to monitor the process when it is faster, which is also more adequate to fit any kinetic model. To this end, the 0.5 mL samples are withdrawn from the top of the reactor with a precision needle and the HPLC vials are prepared with 10 μ L of each sample diluted in 990 μ L acetonitrile.

To study the stability of the biocatalyst, the reaction mixture was filtered using a Buchner filter provided with a 0.47 μ m PTFE membrane to avoid solid losses. The solid was immediately employed for the next reaction cycle. For stability studies, the reaction time was set to 2 h and runs were performed in triplicate. The initial reaction rate was estimated by fitting the FAME concentration curve with time to a hyperbolic growth function and calculating its derivative at zero time. The remaining activity in each cycle was calculated by dividing the initial reaction rate computed for the relevant cycle by the initial reaction rate obtained for the first cycle. Stability was studied for all temperatures and molar ratios tested at 10% *w/w* Lipozyme[®] TL IM.

3.2.2. Analytical Methods

We have adapted a complex gradient RP-HPLC technique using a JASCO HPLC to separate all the relevant families, including mono-, di- and triglycerides, triacetin, ricinoleic acid methyl esters, and other methyl esters. The column employed was a Teknokroma "Mediterranea Sea" C-18 column 25 \times 0.46 cm d_p 5 μ m set in an oven at 30 $^{\circ}$ C and using a flow rate of 1 mL/min. A time-dependent gradient and three eluents were used for the analysis: (A) Water, (B) Acetonitrile, and (C) 2-Propanol-Hexane mixture in volume ratio 5:4 with the following program based on the method proposed by Michal Holcápek et al. [35]:

- At zero time the eluent is: 30% (A) and 70% (B).
- From 0 to 10 min the eluent progressively goes to: 100% (B).
- From 10 to 20 min the eluent progressively changes to: 50% (B) and 50% (C).
- From 20 to 30 min the eluent is: 50% (B) and 50% (C).
- From 30 to 32 min the eluent changes progressively to: 100% (B).
- From 32 to 34 min the eluent progressively changes to: 30% (A) and 70% (B).

A diode array detector (DAD) set at 215 nm was adequate to measure all relevant analytes. The concentrations of the diverse analytes were calculated according to calibration curves obtained with triglycerides and fatty acid methyl esters standards. A typical chromatogram and the calibration lines are included in the Supplementary Material.

3.2.3. Statistical Non-Linear Regression Methods

We have determined the kinetic parameters of this enzymatic interesterification process between castor oil and methyl acetate by fitting a complex kinetic model with six reactions of interesterification combined in series-parallel that take into account all chemical conversions between all the relevant compounds involved. This model is explained in the Section 2 of this paper. We have fitted this model to all experimental data obtained at different concentration and temperature conditions by using a non-linear regression algorithm named NL2SOLV coupled to a numerical integration with a variable step Gauss algorithm applied to the diverse differential equations of the kinetic model. These algorithms are implemented in the software Aspen Custom Modeler v11. As usual, a first fitting process was performed at constant temperature to retrieve the values of the kinetic constants valid at each temperature value. Afterwards, the linearized form of the Arrhenius equation (Equation (7)) is applied to all kinetic constants to obtain values of the neperian logarithms of the pre-exponential factors and the activation energies. In this equation k_i stands for each kinetic constant, $k_{i,0}$ means the preexponential factor of the Arrhenius equation, R is the ideal gases constant -8.31 J/(mol·K), and T is the absolute temperature (K). Finally, a multivariate fitting of the kinetic model is performed using all the available experimental

data. In this case, the temperature was considered an independent variable together with time.

To consider the quality of the model fitting, several physical and statistical criteria have been taken into account [36]. A first physical criterion is the positive value of the kinetic constant when fitting the model to data at a certain temperature. A second physical criterion is an adequate value of the activation energy of any kinetic constant, which should be in the range 20–300 kJ/mol. On its side, all the goodness-of-fit statistical criteria are based on the minimization of the sum of squared residual (SQR), or sum of variances using the y_c values determined with the model for the concentrations of the components and the y_e experimental values of such concentrations. SQR is determined with Equation (9), since this parameter is the base for the calculation of the residual root mean squared error (RMSE), Equation (10), and the Fisher's F value (F), Equation (11). It is evident that if the sum of squared residuals tends to zero, the optimal value, there is a perfect fit of the model to data. In this case, RMSE will take the same value, zero, and the Fisher's F will trend to infinitum. However, to comply with the null-hypothesis, the F-value only has to have a higher value than the threshold value for N data and K parameters. This threshold value for N = 850 data and K = 12 parameters at 95% confidence is 2.725. Any F-value over this value means that the kinetic model proposed is acceptable to fit the considered data.

$$\text{SQR} = \sum_{i=1}^N (y_e - y_c)_i^2 \quad (9)$$

$$\text{RMSE} = \sqrt{\sum_{i=1}^N \frac{(y_e - y_c)_i^2}{(N - K)}} \quad (10)$$

$$F - \text{Fisher} = \frac{\sum_{n=1}^N \frac{(y_c)^2}{K}}{\sum_{n=1}^N \frac{(y_e - y_c)^2}{N - K}} \quad (11)$$

4. Conclusions

The enzymatic interesterification of methyl acetate and castor oil results in mixtures rich in FAMES and, in particular, ricinoleic acid methyl esters, while no glycerol is produced, being the by-product triacetin. In this way, all the reaction components at the end of the process, apart from the excess of methyl acetate, can be used to formulate biodiesel or for higher value-added applications. The operational variables affect the yield to FAME positively, as the increase of temperature, methyl acetate excess, and enzyme concentration result in a very high glycerol conversion and a promising FAME yield at 24 h. Methyl acetate excess is needed to shift all equilibriums towards FAME and the last one towards triacetin, reducing the concentrations of all fatty acid glycerides to levels acceptable for biodiesel formulation. In this sense, an adequate kinetic model is needed for process simulation in a wide range of experimental conditions; a type of model is scarce in literature and non-existent for this reacting system in particular. The kinetic model proposed is based on three second-order reversible reactions in series and fits very accurately to all kinetic data retrieved at the same time. Finally, the presence of methyl acetate helps to alleviate enzyme deactivation at all temperatures, showing Lipozyme[®] TL IM to be a very stable activity when reused for up to five 24-h cycles at temperatures from 40 to 60 °C.

Supplementary Materials: The following supporting information can be downloaded at: <https://www.mdpi.com/article/10.3390/catal12121673/s1>, Figure S1: Typical RP-HPLC chromatogram for the castor oil—triacetin interesterification. Figure S2: Biodiesel (FAME), Triglycerides (TG), Diglycerides (DG) and Monoglycerides (MG) Calibration Graphs. Table S1. Kinetic runs performed for the anhydrous triphasic system; Table S2. Experimental results of the enzymatic esterification of glycerin with ibuprofen immobilized enzyme N435 at T = 50 °C for the anhydrous system; Table S3. Experimental results of the enzymatic esterification of glycerin with ibuprofen immobilized enzyme

N435 at T = 60 °C for the anhydrous system; Table S4. Experimental results of the enzymatic esterification of glycerin with ibuprofen immobilized enzyme N435 at T = 70 °C for the anhydrous system; Table S5. Experimental results of the enzymatic esterification of glycerin with ibuprofen immobilized enzyme N435 at T = 80 °C for the anhydrous system; Table S6. Kinetic runs performed for the hydrated triphasic system; Table S7. Experimental results of the enzymatic esterification of glycerin with ibuprofen immobilized enzyme N435 at T = 50 °C for the system with added water; Table S8. Experimental results of the enzymatic esterification of glycerin with ibuprofen immobilized enzyme N435 at T = 60 °C for the system with added water; Table S9. Experimental results of the enzymatic esterification of glycerin with ibuprofen immobilized enzyme N435 at T = 70 °C for the system with added water; Table S10. Experimental results of the enzymatic esterification of glycerin with ibuprofen immobilized enzyme N435 at T = 80 °C for the system with added water.

Author Contributions: Conceptualization, M.L. and M.E.G.; data curation, A.G.-C. and M.L.; formal analysis, A.G.-C., M.E.G. and M.L.; funding acquisition, M.L.; investigation, A.G.-C.; methodology, M.L.; project administration, M.E.G. and M.L.; resources, M.L.; software, A.G.-C. and M.L.; supervision, M.L.; writing—original draft, M.E.G. and M.L.; writing—review & editing, M.E.G. and M.L. All authors have read and agreed to the published version of the manuscript.

Funding: This research was funded by (1) Ministerio de Ciencia e Innovación of the Government of Spain for financial support of the present research through projects CTQ2017-84963-C2-1-R and PID2020-114365RB-C21 (Spanish Research Agency). (2) Fondo de Investigación Sanitaria, Instituto de Salud Carlos III (ISCIII): PI15/00484, CP16/00046 and PI18/00151 to MEG (co-funded by European Regional Development Fund “A way to make Europe”); PI21/00162 and CPII21/00011 co-funded by the European Union to MEG.

Data Availability Statement: All data will be made available on request.

Acknowledgments: The authors express their thanks to Novozymes A/S for the gift the immobilized enzyme preparation Lipozyme[®] TL IM. In particular we want to express our most sincere gratitude to Novozymes A/S Account Manager Ramiro Martinez for his continued support and guidance.

Conflicts of Interest: The authors declare no conflict of interest.

References

1. Wei, Y.M.; Han, R.; Wang, C.; Yu, B.; Liang, Q.M.; Yuan, X.C.; Chang, J.; Zhao, Q.; Liao, H.; Tang, B.; et al. Self-preservation strategy for approaching global warming targets in the post-Paris Agreement era. *Nat. Commun.* **2020**, *11*, 1624. [[CrossRef](#)] [[PubMed](#)]
2. Desing, H.; Widmer, R.; Beloin-Saint-Pierre, D.; Hischer, R.; Wäger, P. Powering a sustainable and circular economy—An engineering approach to estimating renewable energy potentials within earth system boundaries. *Energies* **2019**, *12*, 4723. [[CrossRef](#)]
3. Zeng, X.; Li, J. Emerging anthropogenic circularity science: Principles, practices, and challenges. *iScience* **2021**, *24*, 102237. [[CrossRef](#)] [[PubMed](#)]
4. Mandari, V.; Devarai, S.K. Biodiesel Production Using Homogeneous, Heterogeneous, and Enzyme Catalysts via Transesterification and Esterification Reactions: A Critical Review. *Bioenergy Res.* **2022**, *15*, 935–961. [[CrossRef](#)]
5. Shokravi, H.; Shokravi, Z.; Heidarzadei, M.; Ong, H.C.; Rahimian Koloor, S.S.; Petrú, M.; Lau, W.J.; Ismail, A.F. Fourth generation biofuel from genetically modified algal biomass: Challenges and future directions. *Chemosphere* **2021**, *285*, 131535. [[CrossRef](#)]
6. Aamer Mehmood, M.; Shahid, A.; Malik, S.; Wang, N.; Rizwan Javed, M.; Nabeel Haider, M.; Verma, P.; Umer Farooq Ashraf, M.; Habib, N.; Syafiuddin, A.; et al. Advances in developing metabolically engineered microbial platforms to produce fourth-generation biofuels and high-value biochemicals. *Bioresour. Technol.* **2021**, *337*, 125510. [[CrossRef](#)]
7. Ma, Y.; Wang, R.; Li, Q.; Li, M.; Liu, C.; Jia, P. Castor oil as a platform for preparing bio-based chemicals and polymer materials. *Green Mater.* **2021**, *40*, 99–109. [[CrossRef](#)]
8. Pasha, M.K.; Dai, L.; Liu, D.; Du, W.; Guo, M. Biodiesel production with enzymatic technology: Progress and perspectives. *Biofuels Bioprod. Biorefining* **2021**, *15*, 1526–1548. [[CrossRef](#)]
9. Monteiro, R.R.C.; Arana-Peña, S.; da Rocha, T.N.; Miranda, L.P.; Berenguer-Murcia, Á.; Tardioli, P.W.; dos Santos, J.C.S.; Fernandez-Lafuente, R. Liquid lipase preparations designed for industrial production of biodiesel. Is it really an optimal solution? *Renew. Energy* **2021**, *164*, 1566–1587. [[CrossRef](#)]
10. Naveenkumar, R.; Baskar, G. Process optimization, green chemistry balance and techno-economic analysis of biodiesel production from castor oil using heterogeneous nanocatalyst. *Bioresour. Technol.* **2021**, *320*, 124347. [[CrossRef](#)]
11. Andrade, T.A.; Errico, M.; Christensen, K.V. Evaluation of Reaction Mechanisms and Kinetic Parameters for the Transesterification of Castor Oil by Liquid Enzymes. *Ind. Eng. Chem. Res.* **2017**, *56*, 9478–9488. [[CrossRef](#)]

12. Wang, L.; Liu, X.; Jiang, Y.; Liu, P.; Zhou, L.; Ma, L.; He, Y.; Li, H.; Gao, J. Silica nanoflowers-stabilized pickering emulsion as a robust biocatalysis platform for enzymatic production of biodiesel. *Catalysts* **2019**, *9*, 1026. [[CrossRef](#)]
13. Wang, L.; Liu, X.; Jiang, Y.; Zhou, L.; Ma, L.; He, Y.; Gao, J. Biocatalytic pickering emulsions stabilized by lipase-immobilized carbon nanotubes for biodiesel production. *Catalysts* **2018**, *8*, 587. [[CrossRef](#)]
14. Hajar, M.; Vahabzadeh, F. Biolubricant production from castor oil in a magnetically stabilized fluidized bed reactor using lipase immobilized on Fe₃O₄ nanoparticles. *Ind. Crops Prod.* **2016**, *94*, 544–556. [[CrossRef](#)]
15. Goswami, D.; Sen, R.; Basu, J.K.; De, S. Surfactant enhanced ricinoleic acid production using *Candida rugosa* lipase. *Bioresour. Technol.* **2010**, *101*, 6–13. [[CrossRef](#)] [[PubMed](#)]
16. Rajalakshmi, P.; Marie, J.M.; Maria Xavier, A.J. Castor oil-derived monomer ricinoleic acid based biodegradable unsaturated polyesters. *Polym. Degrad. Stab.* **2019**, *170*, 109016. [[CrossRef](#)]
17. Zhang, H.; Zhu, F.; Fu, Q.; Zhang, X.; Zhu, X. Mechanical properties of renewable plasticizer based on ricinoleic acid for PVC. *Polym. Test.* **2019**, *76*, 199–206. [[CrossRef](#)]
18. Sun, S.; Guo, J. Enhanced ricinoleic acid preparation using lipozyme TLIM as a novel biocatalyst: Optimized by response surface methodology. *Catalysts* **2018**, *8*, 486. [[CrossRef](#)]
19. Zada, B.; Kwon, M.; Kim, S.W. Current Trends in Acetins Production: Green versus Non-Green Synthesis. *Molecules* **2022**, *27*, 2255. [[CrossRef](#)]
20. Maddikeri, G.L.; Pandit, A.B.; Gogate, P.R. Ultrasound assisted interesterification of waste cooking oil and methyl acetate for biodiesel and triacetin production. *Fuel Process. Technol.* **2013**, *116*, 241–249. [[CrossRef](#)]
21. Patel, V.R.; Dumancas, G.G.; Viswanath, L.C.K.; Maples, R.; Subong, B.J.J. Castor oil: Properties, uses, and optimization of processing parameters in commercial production. *Lipid Insights* **2016**, *9*, LPI-S40233. [[CrossRef](#)] [[PubMed](#)]
22. Pabiś, S.; Kula, J. Synthesis and Bioactivity of (R)-Ricinoleic Acid Derivatives: A Review. *Curr. Med. Chem.* **2016**, *23*, 4037–4056. [[CrossRef](#)] [[PubMed](#)]
23. Dos Santos, D.S.; Piovesan, L.A.; D'Oca, C.R.M.; Hack, C.R.L.; Treptow, T.G.M.; Rodrigues, M.O.; Vendramini-Costa, D.B.; Ruiz, A.L.T.G.; De Carvalho, J.E.; D'Oca, M.G.M. Antiproliferative activity of synthetic fatty acid amides from renewable resources. *Bioorganic Med. Chem.* **2015**, *23*, 340–347. [[CrossRef](#)] [[PubMed](#)]
24. Matysiak, S.; Chmiel, A.; Skolimowski, J.; Kula, J.; Pasternak, B.; Blaszczyk, A. Synthesis and cytotoxicity of (R)- and (S)-ricinoleic acid amides and their acetates. *Chirality* **2017**, *29*, 616–622. [[CrossRef](#)]
25. Park, C.G.; Kim, J.J.; Kim, H.K. Lipase-mediated synthesis of ricinoleic acid vanillyl ester and evaluation of antioxidant and antibacterial activity. *Enzyme Microb. Technol.* **2020**, *133*, 109454. [[CrossRef](#)]
26. Pemha, R.; Kuete, V.; Pagès, J.M.; Pegnyemb, D.E.; Mosset, P. Synthesis and biological evaluation of four new ricinoleic acid-derived 1-o-alkylglycerols. *Mar. Drugs* **2020**, *18*, 113.
27. Mohini, Y.; Prasad, R.B.N.; Karuna, M.S.L.; Poornachandra, Y.; Ganesh Kumar, C. Synthesis and biological evaluation of ricinoleic acid-based lipoamino acid derivatives. *Bioorganic Med. Chem. Lett.* **2016**, *26*, 5198–5202. [[CrossRef](#)]
28. Geesala, R.; Bar, N.; Dhoke, N.R.; Basak, P.; Das, A. Porous polymer scaffold for on-site delivery of stem cells—Protects from oxidative stress and potentiates wound tissue repair. *Biomaterials* **2016**, *77*, 1–13. [[CrossRef](#)]
29. Da Silva, L.P.; Kundu, S.C.; Reis, R.L.; Correlo, V.M. Electric Phenomenon: A Disregarded Tool in Tissue Engineering and Regenerative Medicine. *Trends Biotechnol.* **2020**, *38*, 24–49. [[CrossRef](#)]
30. Xu, Y.; Du, W.; Liu, D. Study on the kinetics of enzymatic interesterification of triglycerides for biodiesel production with methyl acetate as the acyl acceptor. *J. Mol. Catal. B Enzym.* **2005**, *32*, 241–245. [[CrossRef](#)]
31. Sun, S.; Li, K. Biodiesel production from phoenix tree seed oil catalyzed by liquid lipozyme TL100L. *Renew. Energy* **2020**, *151*, 152–160. [[CrossRef](#)]
32. Malani, R.S.; Umriwad, S.B.; Kumar, K.; Goyal, A.; Moholkar, V.S. Ultrasound-assisted enzymatic biodiesel production using blended feedstock of non-edible oils: Kinetic analysis. *Energy Convers. Manag.* **2019**, *188*, 142–150. [[CrossRef](#)]
33. Liu, Y.; Yan, Y.; Hu, F.; Yao, A.; Wang, Z.; Wei, F. Transesterification for biodiesel production catalyzed by combined lipases: Optimization and kinetics. *AIChE J.* **2010**, *56*, 1659–1665. [[CrossRef](#)]
34. Chang, M.Y.; Chan, E.S.; Song, C.P. Biodiesel production catalysed by low-cost liquid enzyme Eversa®Transform 2.0: Effect of free fatty acid content on lipase methanol tolerance and kinetic model. *Fuel* **2021**, *283*, 119266. [[CrossRef](#)]
35. Holčapek, M.; Jandera, P.; Fischer, J.; Prokeš, B. Analytical monitoring of the production of biodiesel by high-performance liquid chromatography with various detection methods. *J. Chromatogr. A* **1999**, *858*, 13–31. [[CrossRef](#)] [[PubMed](#)]
36. Molinero, L.; Ladero, M.; Tamayo, J.J.; García-Ochoa, F. Homogeneous catalytic esterification of glycerol with cinnamic and methoxycinnamic acids to cinnamate glycerides in solventless medium: Kinetic modeling. *Chem. Eng. J.* **2014**, *247*, 174–182. [[CrossRef](#)]